JOURNAL OF VIROLOGY, July 1995, p. 4440–4452 Vol. 69, No. 7
0022-538X/95/$04.00+0

Effects on DNA Synthesis and Translocation Caused by Mutations in the RNase H Domain of Moloney Murine Leukemia Virus Reverse Transcriptase

STACY W. BLAIN† AND STEPHEN P. GOFF*

Howard Hughes Medical Institute, Department of Biochemistry and Molecular Biophysics, College of Physicians and Surgeons, Columbia University, New York, New York 10032

Received 6 February 1995/Accepted 14 April 1995

To determine the various roles of RNase H in reverse transcription, we generated a panel of mutations in the RNase H domain of Moloney murine leukemia virus reverse transcriptase based on sequence alignments and the crystal structures of *Escherichia coli* and human immunodeficiency virus type 1 RNases H (S. W. Blain and S. P. Goff, J. Biol. Chem. 268:23585–23592, 1993). These mutations were introduced into a full-length provirus, and the resulting genomes were tested for infectivity by transient transfection assays or after generation of stable producer lines. Several of the mutant viruses replicated normally, some showed significant delays in infectivity, and others were noninfectious. Virions were collected, and the products of the endogenous reverse transcription reaction were examined to determine which steps might be affected by these mutations. Some mutants left their minus-strand strong-stop DNA in RNA-DNA hybrid form, in a manner similar to that of RNase H null mutants. Some mutants showed increased polymerase pausing. Others were impaired in first-strand translocation, independently of their wild-type ability to degrade genomic RNA, suggesting a new role for RNase H in strand transfer. DNA products synthesized in vivo by the wild-type and mutant viruses were also examined. Whereas wild-type virus did not accumulate detectable levels of minus-strand strong-stop DNA, several mutants were blocked in translocation and did accumulate this intermediate. These results suggest that in vivo wild-type virus normally translocates minus-strand strong-stop DNA efficiently.

The conversion of the single-stranded RNA genome of a retrovirus to a double-stranded DNA copy involves several complex steps, which are mediated by the viral reverse transcriptase (RT) (2, 64). RT carries out this conversion by using two main activities: a DNA polymerase activity which is able to synthesize DNA from both RNA and DNA templates and an RNase H activity which is able to degrade RNA present in RNA-DNA hybrid form (for reviews, see references 14, 26, 34, 57, and 68). The two activities of Moloney murine leukemia virus (M-MuLV) RT reside in separable domains: the DNA polymerase domain lies in the N-terminal two-thirds of the enzyme, while the RNase H domain is in the C-terminal third (59). The RNase H domain of M-MuLV RT is highly homologous with other RNases H, including those of *Escherichia coli* (39, 70) and human immunodeficiency virus type 1 (HIV-1) (15, 35, 40). Thus, it is likely that the structure of the RNase H domain of this enzyme will be similar to those of other RNases H (46). However, the extent and nature of the contacts between the DNA polymerase and RNase H domains of the murine enzyme are not yet known.

RNase H activity has been implicated in several steps in reverse transcription and is essential for the viral life cycle, as mutant viruses which lack RNase H activity are noninfectious (60). Reverse transcription of the viral genome is initiated at a tRNA primer bound to a region near the 5′ end of the genomic RNA, termed the primer binding site (PBS). Elongation of the tRNA to the 5′ end of the genome results in formation of minus-strand strong-stop DNA, the first DNA intermediate to appear during reverse transcription (11). This species must then translocate to the opposite end of the template RNA to continue minus-strand synthesis. Transfer can be either intramolecular to the 3′ end of the same template or intermolecular to the 3′ end of the other identical RNA packaged in the virion (31, 36, 49). The translocation is facilitated by the presence of a short repeated sequence at both the 5′ and the 3′ ends of the viral RNA, called the R region, which promotes base pairing between the minus-strand strong-stop DNA and the 3′ RNA acceptor template. RNase H is thought to degrade the 5′ portion of the genomic RNA in hybrid form with the newly synthesized minus-strand strong-stop DNA. Analysis of abortive replication products produced by virions which lack RNase H has shown that the minus-strand strong-stop DNA remains in hybrid RNA-DNA form with the genomic RNA, blocking translocation and further elongation (60). In addition to degradation of the genomic RNA, RNase H performs several specialized functions, including the creation and removal of the polypurine tract primer and the removal of the minus-strand tRNA primer (9).

While the DNA polymerase and RNase H activities of M-MuLV RT are separable in vitro, we are learning that mutations in the RNase H domain can affect DNA polymerase activity. It has been shown in vitro that some RNase H mutations affect both DNA processivity and the interactions of RT with its primer template, suggesting that the two domains and activities may act together during the course of reverse transcription, both functionally and structurally (61, 62, 69). The ΔRH form of M-MuLV RT, completely missing the RNase H domain, is less processive on both homopolymeric and heteropolymeric substrates (3, 62).

To determine the effect of mutation of the RNase H domain of M-MuLV RT on reverse transcription, we generated a panel

* Corresponding author. Mailing address: Howard Hughes Medical Institute, Department of Biochemistry and Molecular Biophysics, College of Physicians and Surgeons, Columbia University, 701 W. 168th St., New York, NY 10032. Phone: (212) 305-3794. Fax: (212) 305-8692.

† Present address: Department of Cell Biology and Genetics, Memorial Sloan-Kettering Cancer Center, New York, NY 10021.

of mutants based on sequence alignments and the crystal structures of *E. coli* and HIV-1 RNases H and the predicted structure of the M-MuLV RNase H domain (5). This mutagenesis targeted specific residues which might be involved in substrate binding, while attempting to affect only minimally the overall folding of the protein. We believed that we might be able to alter the enzymatic properties of M-MuLV RT without abolishing catalytic activity or to affect a specific step in the viral life cycle. We previously characterized these mutant enzymes expressed in *E. coli* for DNA polymerase activity on oligo(dT)-poly(rA) primer templates and for nuclease activities on both RNA-DNA and RNA-RNA substrates by using in situ gel techniques (5). The bulk of these RT mutants retained significant RNase H activity in vitro, with many of the mutants having wild-type or near wild-type activity on the heteropolymeric substrate tested. In this report, we assess the biological activity of these mutant viruses.

MATERIALS AND METHODS

Construction of mutants. M-MuLV mutant RTs were constructed by oligonucleotide-mediated site-directed mutagenesis as previously described (5). Eight point mutations, D-524 to N (D524N), S526A, Q530N, AQ558NN, Y586F, Y598V, FL625GA, R657S, and Δ5E, a 5-amino-acid deletion from S-643 to R-647, were subcloned into pNCA, a cloned copy of the infectious Moloney murine leukemia provirus (12). The mutant enzymes were named by appending the amino acid present in wild-type RT, the residue number, and the amino acid present in the mutant at this position. H7 is a linker insertion mutant, containing a frameshift at the start of the RNase H domain, and thus is effectively an RNase H null virus (59, 60); ΔC has an 11-amino-acid deletion from I-593 to L-603 in the RNase H domain (5, 61). Δ5E and ΔC removed sequences in M-MuLV RNase H that were missing in either the *E. coli* or the HIV-1 enzymes.

Cells, virus, and DNA-mediated transformations. NIH 3T3 cells were maintained in Dulbecco modified Eagle medium supplemented with 10% calf serum as previously described (60). Viral DNAs were tested for replication competence by transformation of NIH 3T3 cells by the DEAE-dextran method (45). Production of infectious virus and subsequent viral spread were assessed by measuring RT activity in the culture supernatant medium by the oligo(dT)-poly(rA) primer template assay (27). Stable viral producer lines were generated for several proviral DNAs. These lines were cloned as single cells from populations of NIH 3T3 cells which were subjected to calcium phosphate-mediated cotransformation with a mixture of proviral and pSV2his DNA; recipient cells were selected with 1.07 mg of L-histidinol (Sigma, St. Louis, Mo.) per ml (28, 67). Virion proteins were analyzed by Western blot (immunoblot) analysis with anti-30-2, an anti-RT polyclonal rabbit antibody (5). Low-molecular-weight, preintegrative DNA was isolated at various times postinfection and processed as described previously (29). The procedure was modified by the addition of proteinase K (200 μg/ml) for 45 min at 55°C to the clarified lysate prior to phenol extraction. Viral DNA sequences were detected either by agarose gel electrophoresis and Southern blot analysis or by PCR amplification with primers complementary to pNCA sequences. Primers 5′EcoRV (5′CCCGGCTACGCTGCTCCC3′) and 3′Int (5′GGCCCCCAACTTGGTTAGG3′) were used to amplify the entire RNase H domain from nucleotide (nt) 4482 to 5138, by standard PCR techniques (25 cycles with an annealing temperature of 57°C). Infection with virus in the presence of Polybrene was performed as previously described (60). To prepare virions, producer cells were fed with Dulbecco modified Eagle medium supplemented with 10% NuSerum (Collaborative Biomedical Products, Bedford, Mass.) for 12 h prior to harvest. The virions were first pelleted for 3 h at 25,000 rpm and then resuspended, layered over a 25 to 45% sucrose step gradient, and sedimented to the interface. The viral band was collected and repelleted for 2 h at 25,000 rpm following dilution in TNE (50 mM Tris-HCl [pH 7.5], 100 mM NaCl, 1 mM EDTA).

Endogenous RT reactions. Endogenous reactions using concentrated virions were performed under two different sets of conditions. To detect long minus-strand DNA products, reaction mixtures were incubated for >1 h at 37°C in buffer (50 mM Tris-Cl [pH 8.3], 50 mM NaCl, 6 mM $MgCl_2$, 0.01% Nonidet P-40, 1 mM dithiothreitol) in the presence of 100 μg of actinomycin D per ml and 2 mM (each) dCTP, dATP, and dGTP and 1 mM [α-^{32}P]TTP at 1 Ci/mmol (60). To detect minus-strand strong-stop products, reaction mixtures were incubated for <30 min at 37°C in a lower concentration of nucleotides (1 mM [each] dATP, dGTP, and dCTP and 2.5 μM [α-^{32}P]TTP at 400 Ci/mmol) as previously described (60). Reaction products were treated with sodium dodecyl sulfate (SDS) and proteinase K for 15 min at 37°C, phenol extracted, and ethanol precipitated in the presence of carrier tRNA. Products were then treated with RNase A (80 μg/ml) at 37°C for 30 min or with 0.33 N NaOH at 55°C for 30 min before the final ethanol precipitation to remove RNA primers. Reaction products were analyzed on 7.5% denaturing polyacrylamide gels. Nonradiolabeled endogenous reactions were performed in the presence of 100 μg of actinomycin D per ml and 2 mM (each) dCTP, dATP, dGTP, and TTP, and products were processed as described above.

Translocation assays. To analyze translocation quantitatively, we performed RNase protection assays against minus-strand viral DNAs either synthesized in vitro in the endogenous reaction or synthesized in vivo following viral infection and harvested as low-molecular-weight, preintegrative DNA. Briefly, the probe consisted of a radiolabeled, plus-strand RNA mapping at the 5′ end of the retroviral genome from *Msc*I (position 662) to *Sac*I (position 414) in pNCA, which includes the U5 and R regions and part of the U3 region of the M-MuLV long terminal repeat. This probe was hybridized with nonradiolabeled minus-strand DNA and treated with a mixture of RNases A and T1, under standard RNase protection conditions (Ambion, Austin, Tex.). When endogenous reaction products were protected, we were able to differentiate between minus-strand strong-stop DNA (giving a 145-nt fragment) and longer translocated products (giving a 185-nt fragment). When low-molecular-weight preintegrative DNA, harvested at various time points postinfection, was protected, we were able to differentiate between minus-strand strong-stop, translocated, and full-length complete minus-strand DNA (giving a 242-nt fragment). Following RNase digestion for 2 h at 30°C, the products were treated with SDS and proteinase K for 15 min at 37°C, phenol extracted, ethanol precipitated, and analyzed in formamide loading buffer following heating at 85°C for 10 min on 7.5% denaturing polyacrylamide gels.

Enzyme digestions of labeled DNA species. To determine the nature of the minus-strand strong-stop DNA, high-specific-activity endogenous reaction products were treated with RNase A (2 μg in 50 μl) in either a low-salt (Tris-EDTA [TE]) or a high-salt (TE containing 0.5 M NaCl) buffer for 30 min at 37°C, as previously described (60). The enzyme was inactivated by diethylpyrocarbonate treatment, and the products were phenol extracted and ethanol precipitated in the presence of carrier tRNA. The samples were then either diluted into electrophoresis sample buffer and solubilized without denaturation by mild heating (50°C for 5 min) or diluted into buffer containing formamide and fully denatured (90°C for 10 min). The samples were then analyzed on 7.5% nondenaturing polyacrylamide gels.

To recover DNA from wet gels, the DNA was electroeluted in dialysis bags in 0.25× TBE buffer, ethanol precipitated, and resuspended in TE containing 2 μg of carrier tRNA. The recovered DNAs were analyzed by electrophoresis on either nondenaturing or denaturing gels, with or without additional RNase A treatment. The DNAs also were analyzed by standard S1 nuclease mapping and RNase protection procedures (55). The excised forms were treated with DNase I to remove the radiolabeled minus-strand DNA, and the plus-strand, genomic RNA was analyzed by RNase protection with a minus-strand probe which contained pNCA sequences from the *Msc*I site (position 662) 3′ of the PBS to the *Asp*718 site (position 481) in U5.

RESULTS

Test for viral replication. A series of mutations in the RNase H domain were transferred into the full-length M-MuLV provirus, pNCA (12). The cloned proviral DNAs were introduced into NIH 3T3 cells in culture by using DEAE-dextran. Viral spread was detected by assaying for RT activity in the culture supernatant. As summarized in Table 1 and shown in Fig. 1A, three mutant viruses, Q530N, AQ558NN, and FL625GA, which displayed wild-type activities in vitro, were as infectious as the wild type. Thus, these three mutations had no detectable effect on RT function in vivo.

Three mutant viruses, S526A, R657S, and Y598V, which all were found to retain significant RNase H activity when assayed in vitro (25, 100, and 100% of the wild-type activity, respectively), showed delays in the rate of viral spread following DEAE-dextran transient transfection (Fig. 1A). Virus was normalized by the amount of virion-associated RT activity and used to infect fresh NIH 3T3 cells, to address the possibility that these mutant viruses might have undergone reversion or recombination events. Since all of the mutant RTs had previously been shown to have wild-type DNA synthesis on oligo(dT)-poly(rA) primer templates, normalization by RT activity was appropriate (5). All three viruses still had the same phenotypes following infection: significant delays in the rate of RT appearance compared with fully infectious wild-type virus (Fig. 1B). Low-molecular-weight, preintegrative DNA was harvested at 24 h postinfection and analyzed by PCR amplification, using primers which would amplify a portion of the *pol* coding region. In all three cases the original mutation was still

TABLE 1. Analysis of RNase H mutant viruses

Mutant	RNase H activity (%)[a]	Delay of release of progeny virus beyond wild type		Major −sss species[b]	Translocated minus-strand products[c]	Nature of −sss DNA[d]	Translocation[e]
		Transfection[f]	Infection[g]				
D524N	10–25	Dead	Dead	+	Reduced	Hybrid	ND
Y586F	5	Dead	Dead	+	Reduced	Hybrid	ND
Δ5E	50	Dead	Dead	+	Reduced	Hybrid	ND
ΔC	100	Dead	Dead	Truncated	Reduced	Hybrid	ND
H7	<1	Dead	Dead	Truncated	Reduced	Hybrid	ND
R657S	100	~5	~20	Reduced	Reduced	SS	+
S526A	25	~2	~8	+	Reduced	SS	Reduced
Y598V	100	~12	~30	+	Reduced	SS	Reduced
Q530N	100	WT					
AQ558NN	100	WT					
FL625GA	100	WT					

[a] Mutants were assayed in vitro for RNase H activity by in situ gel techniques, as previously described (5). Activities are expressed as percentages of wild-type activity, where wild-type RT activity is 100%.

[b] Products detected in the endogenous reaction. +, full-length minus-strand strong-stop (−sss) DNA; Truncated, truncated −sss DNA due to increased RT pausing; Reduced, reduced levels of full-length −sss DNA.

[c] Levels of longer, translocated minus-strand products detected in the endogenous reaction. Reduced, reduced levels of longer products.

[d] Hybrid or single-stranded (SS) −sss DNA, as assayed by RNase A treatment, S1 nuclease analysis, and RNase protection.

[e] Levels of first-strand transfer detected both in vitro and in vivo by RNase protection of endogenous reaction products and low-molecular-weight, preintegrative DNA. +, wild-type (WT) transfer levels; Reduced, reduced transfer levels; ND, not determined.

[f] Mutant proviral DNAs were assayed for infectivity by DEAE-dextran transient transfection. Supernatant was harvested and analyzed for RT activity as a measure of viral spread. Dead, no RT activity after multiple passages; WT, RT positive the same day as pNCA. Numbers indicate delays of appearance of RT (in days) beyond the time of RT appearance for pNCA.

[g] Mutant virus harvested from stable producer lines was assayed by infection. Dead, no RT activity after multiple passages. Numbers are as described in footnote *f*.

present (data not shown), ruling out the possibility of reversion at the site of the mutation. The presence of the original mutation and the appearance of a similar delay in viral spread following repeated infection suggested that these mutants had not reverted but rather were impaired in some aspect of viral replication.

Viral spread was not detected for Δ5E, Y586F, and D524N even after 6 weeks of passage (Fig. 1A). These mutations completely blocked replication. Y586F and D524N had little RNase H activity in vitro as assayed by in situ gel techniques, consistent with the replication-defective phenotypes detected in vivo (Table 1). Δ5E, however, retained 50% of the wild-type RNase H activity in vitro, and so its blocked replication was surprising.

Construction of stable virus-producing cell lines. Stable cell lines that produced RT-positive virions harboring the partially replication-defective mutants, S526A, R657S, and Y598V, were established by the calcium phosphate cotransformation method, with pSV2his as a selectable marker. Virions shed from these lines were normalized by RT oligo(dT)-poly(rA) primer template assays, and equivalent amounts of virus were used to infect NIH 3T3 cells. Low-molecular-weight, preintegrative viral DNA was harvested at 24 h postinfection and analyzed by Southern blot analysis (Fig. 2 and data not shown). S526A, R657S, and Y598V were reduced at least 100-fold in viral DNA levels compared with the wild type (Fig. 2, lanes 5 to 8, and data not shown). Thus, these RNase H mutants, which retained significant RNase H activity in vitro, were impaired in some aspects of viral replication in vivo. This suggested that the role of RNase H in reverse transcription might involve more than RNA degradation.

Stable cell lines harboring Δ5E, D524N, and Y586F mutations similarly were established by the calcium phosphate method, also with pSV2his as a selectable marker. Virions from these lines were tested along with virions harvested from two previously described producer cell lines containing the RT mutations H7 and ΔC (60, 61). When virions from the Δ5E, D524N, and Y586F cell lines were applied to NIH 3T3 cells, they were found still to be noninfectious, with no progeny virus released. Low-molecular-weight, preintegrative viral DNA was harvested at 24 h postinfection and analyzed by Southern blot analysis (Fig. 2 and data not shown). D524N and Δ5E did not produce any detectable DNA (Fig. 2, lanes 3 and 4, and data not shown). Y586F made very low levels, at least 100-fold lower than those of the wild type (Fig. 2, lanes 1 and 2). H7 and ΔC viruses were also noninfectious and did not produce any detectable low-molecular-weight, preintegrative DNA, as has been previously described (60, 61).

Analysis of virion proteins. Virions from the three replication-delayed viruses (S526A, R657S, and Y598V) and the five noninfectious viruses (Δ5E, Y586F, D524N, H7, and ΔC) were isolated from culture medium of stable producer cells. The virions were examined by Western blot analysis using anti-30-2, an anti-RT polyclonal antibody (5), and all were found to contain an RT product of the correct size (72 kDa for most mutants; examples are shown in Fig. 3). This result suggests that all the mutants produce substantial levels of *pol* gene products and package and process these proteins normally. R657S also had a prominent species of about 65 kDa, in addition to the full-length 72-kDa species (Fig. 3, lane 1). Analysis of the recombinant R657S expressed in *E. coli* also revealed a 65-kDa proteolytic fragment, which had RNA-DNA nuclease activity (5). The exact structure of this proteolytic species was not determined. All of the mutants and the wild type had various amounts of an approximately 50-kDa species, reactive with the anti-RT antiserum, which presumably corresponds to another RT breakdown product. The exact structure of this species is unknown, but its presence in purified virions has been previously detected (30). Western blot analysis of pRT30-2, the *E. coli*-expressed wild-type RT, also resulted in the detection of an approximately 50-kDa RT-specific breakdown product (5).

Reverse transcription by mutant virions in vitro: the endogenous reaction. To define the nature of the defects conferred by these mutations, we examined the replication products produced in the endogenous RT reaction. When concentrated

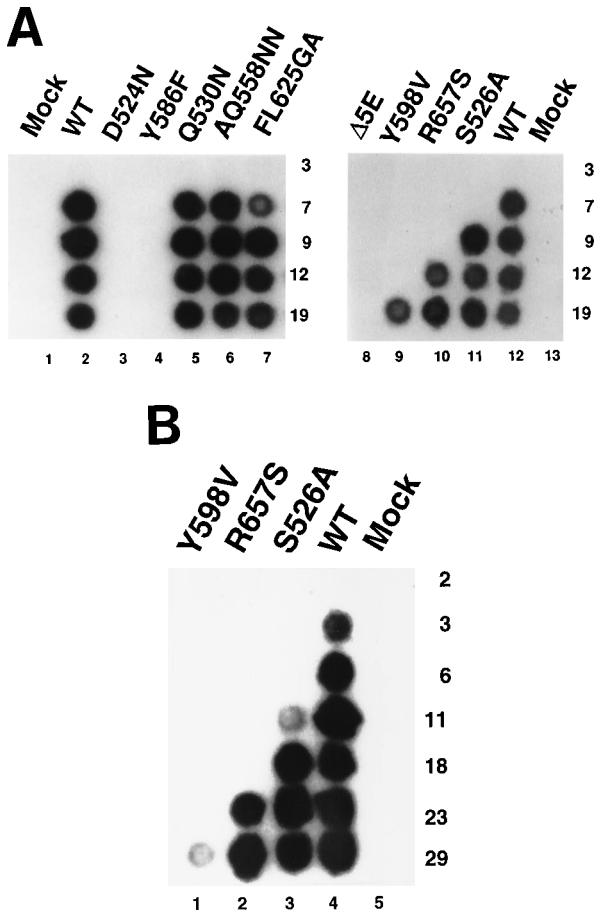

FIG. 1. Test of viral DNA and virus infectivity. (A) Proviral DNAs were analyzed for infectivity by DEAE-dextran transient transfection in NIH 3T3 cells. Mock, mock transfection; WT, wild-type pNCA. Culture supernatant was harvested at 3, 7, 9, 12, and 19 days posttransfection and analyzed for RT activity as a measure of viral spread. (B) Virus was quantitated by RT activity and used to infect NIH 3T3 cells. WT, wild type; Mock, mock infection. Culture supernatant was harvested at 2, 3, 6, 11, 18, 23, and 29 days postinfection and analyzed for RT activity as a measure of viral spread.

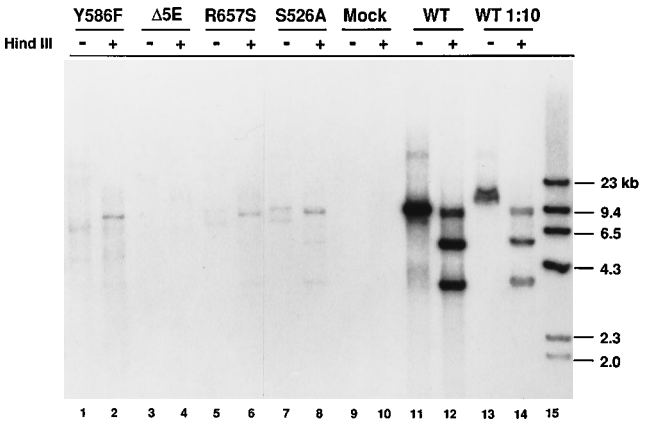

FIG. 2. Southern analysis of low-molecular-weight, preintegrative DNA. Low-molecular-weight, preintegrative viral DNA was harvested at 24 h postinfection and processed as described in Materials and Methods. The viral DNA sequences were detected by agarose gel electrophoresis and Southern blot analysis, using a pNCA randomly primed, radiolabeled DNA probe. Viral DNA was digested with *Hin*dIII, which cleaves viral DNA sequences within the *pol* coding region (lanes 2, 4, 6, 8, 10, 12, and 14). Digestion of wild-type (WT) DNA results in the production of three bands of approximately 8, 5.3, and 3.5 kb. The 8-kb band is derived from cleavage of 1 or 2 long terminal repeat circular forms, while the 5.3- and 3.5-kb bands are derived from cleavage of linear, full-length viral DNA. Mock, mock infection; WT, wild-type pNCA infection. Lanes 13 and 14 correspond to a wild-type infection with a titer 10-fold lower than that for lanes 11 and 12.

M-MuLV virions are permeabilized with 0.01% Nonidet P-40 in the presence of deoxyribonucleotides, various DNA intermediates can be detected. Reactions carried out for >1 h in high nucleoside triphosphate concentrations (1 mM TTP at 1 Ci/mmol) allow translocation of minus-strand strong-stop DNA and formation of longer minus-strand products (Fig. 4) (25, 53, 54). Reactions were performed in the presence of 100 μg of actinomycin D per ml, so that synthesis was limited to minus-strand DNA. Equal amounts of virions were assayed, as quantitated by RT activity and Western blot analysis. With wild-type virions, the 145-nt minus-strand strong-stop DNA was detected, and large amounts of long DNAs were formed, indicating efficient translocation and elongation of the minus-strand strong-stop DNA (Fig. 4A, lane 6; Fig. 4B, lane 3). Longer minus-strand products are seen as a smear at the top of the gel, because the various-sized species cannot be resolved in this gel system. R657S, Δ5E, Y598V, S526A, Y586F, and D524N also all synthesized the full-length 145-nt species, but they showed reduced amounts of longer, translocated products (Fig. 4A, lanes 1 to 3 and 7; Fig. 4B, lanes 1 and 2). This result suggests that these six mutants were significantly impaired either in strand elongation following translocation or in translocation itself.

The total amounts of minus-strand strong-stop DNA detected for mutants ΔC and H7 were reduced (Fig. 4A, lanes 4 and 5; longer exposure in lanes 8 and 9). For H7, low levels of full-length minus-strand strong-stop DNA could be detected, but shorter species were predominantly detected. Mutant ΔC did not make any detectable 145-nt minus-strand strong-stop DNA, but it did synthesize a predominant species that migrated at approximately 67 nt. Several prominent pauses are visible for all the virions assayed, though the pauses appear to different extents for different mutants. This result suggests that H7 and ΔC might be impaired in DNA elongation. Low levels of longer minus-strand products can be seen at the top of the

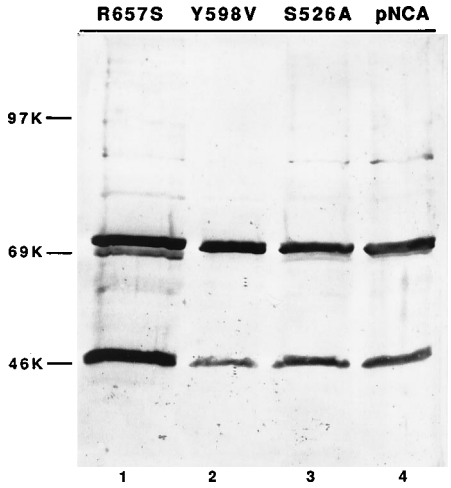

FIG. 3. Western analysis of viral RTs. Anti-30-2 polyclonal antibody was used to analyze virion-associated RTs. The same amount of RT was analyzed for each lane, as determined by RT activity in the oligo(dT)-poly(rA) primer template assay. Virions were boiled in SDS loading buffer for 5 min and then forced through a Hamilton syringe prior to loading.

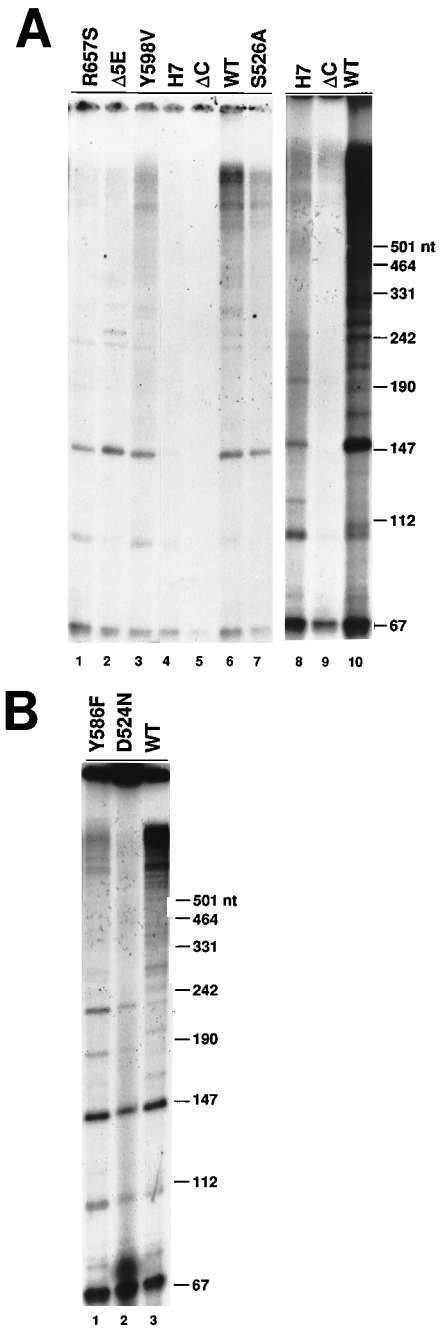

FIG. 4. Reverse transcription in vitro in the endogenous reaction. (A) The endogenous reaction was performed as described in Materials and Methods with 1 mM [α-^{32}P]TTP. WT, wild-type pNCA. Lanes 8 to 10 correspond to a longer exposure of lanes 4 to 6 to allow H7 and ΔC to be visualized. (B) The same reaction was performed with different mutants.

gel for H7, implying that even this mutant can translocate to some extent (Fig. 4A, lane 8). This low-level but detectable translocation may result from breathing at the end of the template, which would transiently expose the minus-strand strong-stop DNA for base pairing and subsequent elongation.

Enzyme digestions of labeled DNA species: single-stranded versus hybrid minus-strand strong-stop DNA. Previous work has shown that RNase H null mutants are noninfectious and that their minus-strand strong-stop DNA is not efficiently translocated and elongated (60). This translocation defect probably results from the inability of these mutant RNases H to degrade their genomic RNA present in RNA-DNA hybrid form. By leaving minus-strand strong-stop DNA in double-stranded form, the requisite base pairing between the complementary R regions at the 3′ end of the minus-strand strong-stop DNA and the 3′ end of the genomic RNA is prevented. To test whether some of our mutants might also leave their minus-strand strong-stop DNA in hybrid form, we examined the nature of the minus-strand strong-stop DNA itself (60). Briefly, the endogenous reaction was performed for 30 min at 37°C in low nucleoside triphosphate concentrations. The products were then treated with RNase A in either low (TE) or high (0.5 M NaCl) salt concentrations. RNase A treatment in high salt concentrations will digest only single-stranded RNA, leaving intact any RNA that is present in hybrid or duplex form. Treatment of DNA from RNase H null mutant virions with RNase A in high salt concentrations will result in the formation of a perfect hybrid of 163 bp, which will migrate as a fast form (FF) on a nondenaturing polyacrylamide gel. However, treatment of wild-type products with RNase A in high salt concentrations, in which most of the genomic RNA has been degraded by RNase H, will result in the formation of a mostly single-stranded form (SF), which migrates very slowly on the same nondenaturing polyacrylamide gel. These species can be further examined after heat treatment to denature any hybrids.

RNase A analyses were performed on wild-type controls and each of the mutant viruses. Treatment of wild-type products with RNase A in high salt concentrations resulted in the formation of the expected slowly migrating form (SF; Fig. 5, lane 9). Upon denaturation, the SF species was chased to a 163-nt form (Fig. 5, lane 10). This corresponds to the 145-nt minus-strand strong-stop DNA plus 18 nt of the tRNA primer, which was resistant to cleavage because it was present in duplex form with the genomic PBS. Analysis of mutant Δ5E, however, resulted in the formation of very little of the slow form and the appearance of the fast form (FF; Fig. 5, lane 1). Upon denaturation, the mutant FF species also was converted to a 163-nt form (Fig. 5, lanes 2 and 6), showing that the minus-strand strong-stop DNA was full length. Treatment with RNase A in low salt concentrations of both wild-type and Δ5E DNAs resulted in a 145-nt species with or without denaturation, corresponding to the full-length minus-strand strong-stop DNA, devoid of the tRNA primer, and confirming that this DNA was intact (Fig. 5, lanes 3, 4, 11, and 12).

The nature of these forms was additionally analyzed by S1 nuclease digestion. The slow and fast forms produced by digestion with RNase A in high salt concentrations were excised from wet gels, electroeluted, and subjected to S1 nuclease analysis (Fig. 6). In all cases, S1 treatment of the fast form resulted in full protection of a 163-nt species (from Δ5E; Fig. 6, lanes 13 and 14), and treatment of the slow form resulted in complete digestion of this species (from the wild type; Fig. 6, lanes 7, 8, 11, and 12). This verified that the slow and fast forms are single and double stranded, respectively. Additional pieces of RNA, resulting from incomplete RNase H digestion, which may still be bound to the 163-nt DNA, are presumed to cause the slower migration of the SF species. The genomic PBS region is an example of an RNA species which may remain annealed to the minus-strand strong-stop DNA. However, we did not observe protection of smaller species in the S1 nuclease analysis, suggesting that these RNAs are very small and/or heterogeneous.

Two other mutants (D524N and Y586F) also generated the FF species upon treatment with RNase A and high salt concentrations, suggesting that in the setting of the endogenous

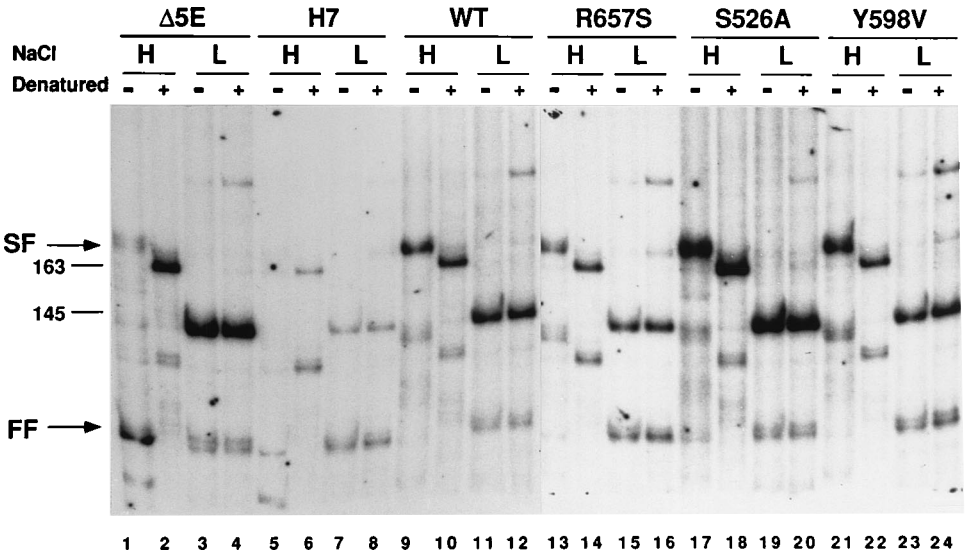

FIG. 5. RNase A treatment of endogenous reaction products in high and low salt concentrations. The endogenous reaction was performed as described in Materials and Methods with 2.5 μM [α-^{32}P]TTP at 400 Ci/mmol. WT, wild type. The products were treated with RNase A in high-salt (H) or low-salt (L) buffer prior to electrophoresis on 7.5% nondenaturing polyacrylamide gels. Lanes 2, 4, 6, 8, 10, 12, 14, 16, 18, 20, 22, and 24 were denatured prior to loading by suspension in dye containing formamide. Lanes 1, 3, 5, 7, 9, 11, 13, 15, 17, 19, 21, and 23 were analyzed without denaturation.

reaction these RNases H were inactive and that they were effectively RNase H null mutants (Fig. 7A, lane 3, and Fig. 7B, lane 9). Denaturation of these FF species produced the 163-nt full-length minus-strand strong-stop DNA species (Fig. 7A, lane 4; Fig. 7B, lane 10). Treatment with RNase A in low salt concentrations produced the 145-nt species (Fig. 7A, lanes 5 and 6; Fig. 7B, lane 11). Treatment of the excised FF species from D524N and Y586F with S1 nuclease resulted in protection of the 163-nt form (Fig. 6, lanes 9 and 10, and data not shown). Thus, the reduction in the levels of longer translocated minus-strand products for D524N, Y586F, and Δ5E was probably due to the retention of the minus-strand strong-stop DNA in hybrid form.

Mutants S526A, R657S, and Y598V, treated with RNase A in high salt concentrations, produced predominantly the slow, single-stranded SF species, implying that these mutant RNases H were able to efficiently degrade their genomic RNA (Fig. 5, lanes 13, 17, and 21). Denaturation of this SF species resulted in the full-length 163-nt form (Fig. 5, lanes 14, 18, and 22). Treatment in low salt concentrations resulted in the 145-nt species with or without denaturation (Fig. 5, lanes 15, 16, 19, 20, 23, and 24). S1 nuclease treatment of the R657S, S526A, and Y598V SF species resulted in complete digestion of the 163-nt form (Fig. 6, lanes 1 to 6). Thus, the reduction in the levels of longer, translocated minus-strand products for these mutants was not due to retention of the minus-strand strong-stop DNA in hybrid form. This suggested that these mutants must have an additional defect in strand translocation itself, independent of RNA degradation. We noted, however, that mutant R657S appeared to have overall synthesis levels slightly lower than those of the wild type and the other mutants (Fig. 4A, lane 1; Fig. 5, lanes 13 to 16).

Truncated minus-strand strong-stop DNA forms. H7 and ΔC mutants showed severe reductions in full-length minus-strand strong-stop DNA levels (Fig. 4A, lanes 4 and 5; Fig. 5, lanes 5 to 8). The presence of shorter DNA products in the endogenous reaction suggests that these mutants may pause prematurely before reaching the end of the genomic template (Fig. 4A, lanes 8 and 9). In vitro analysis of a ΔRH form of RT and mutant ΔC has suggested that deletion or mutation of the RNase H domain may decrease RT's processivity (62). Treatment of ΔC and H7 endogenous reaction products with RNase A in high salt concentrations resulted in the detection of a prominent new species (VFF), which migrated even faster on a nondenaturing polyacrylamide gel (Fig. 7A, lane 1; Fig. 7B, lane 5; Fig. 8A, lane 5). This species is also weakly seen with the other mutants and the wild type, but it is the most prominent product synthesized by both H7 and ΔC virions (Fig. 7A, lane 7; Fig. 7B, lanes 1 and 9; Fig. 8A, lanes 3 and 4). This very fast form (VFF) was excised from the wet gel, electroeluted, ethanol precipitated, and then subjected to additional RNase A treatment in both high and low salt concentrations. Additional RNase A treatment in high salt concentrations did not change this species (Fig. 8A, lane 6), but denaturation pro-

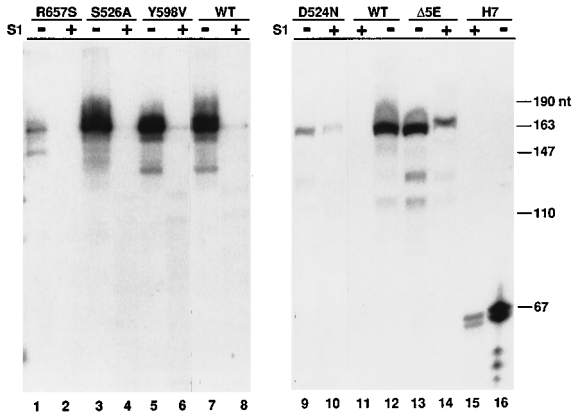

FIG. 6. S1 nuclease analysis of endogenous reaction products. Radiolabeled minus-strand strong-stop DNA products from the endogenous reaction were excised from wet gels after electrophoresis and overnight exposures to X-ray film, to establish the position of the DNA species, and then subjected to S1 nuclease treatment as described in Materials and Methods. These reactions were analyzed on 7.5% denaturing polyacrylamide gels. WT, wild type. Minus-strand strong-stop DNAs were analyzed, with (+) or without (−) S1 nuclease treatment.

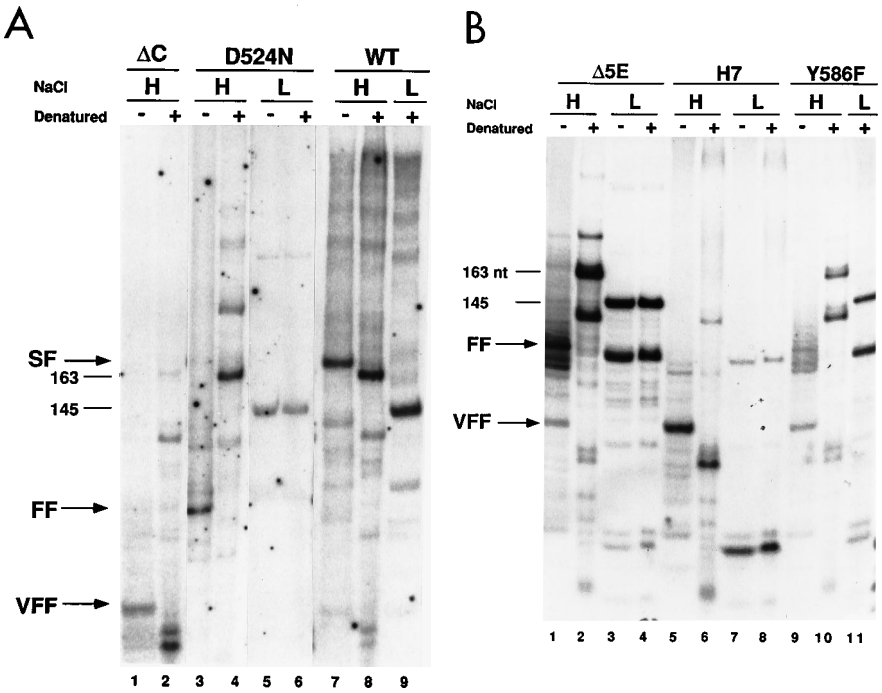

FIG. 7. RNase A treatment of endogenous reaction products in high and low salt concentrations. (A) The endogenous reaction was performed as described in Materials and Methods with 2.5 μM [α-^{32}P]TTP at 400 Ci/mmol. WT, wild type. The products were treated with RNase A in high (H) or low (L) salt concentrations prior to electrophoresis on 7.5% nondenaturing polyacrylamide gels. Lanes 2, 4, 6, 8, 9 were denatured prior to loading by suspension in dye containing formamide. Lanes 1, 3, 5, 7 were analyzed without denaturation. (B) The same reaction was performed with different mutants, and products were treated in the same way. Lanes 2, 4, 6, 8, 10, and 11 were denatured prior to loading by suspension in dye containing formamide. Lanes 1, 3, 5, 7, and 9 were analyzed without denaturation.

duced a fast-migrating doublet (Fig. 8A, lane 7). RNase A treatment of the VFF species in low salt concentrations resulted in an even faster migrating doublet, which did not change upon denaturation (Fig. 8A, lanes 8 and 9). This last result suggests that the VFF species produced by ΔC and H7 is a short DNA in duplex form and is tRNA primed and that low-salt RNase A treatment removes this RNA primer. These forms also can be seen with ΔC and H7 virions analyzed without excision and additional RNase A treatment (Fig. 7A, lanes 1 and 2; Fig. 7B, lanes 5 to 8).

To confirm that the VFF species was actually a M-MuLV-templated DNA form, we analyzed this product by RNase protection with an M-MuLV-specific probe (Fig. 8B). The SF(WT), FF(Δ5E), and VFF(H7) species were purified from the gel and treated with DNase I to remove the radiolabeled minus-strand DNA, and the genomic RNA was analyzed by RNase protection with a minus-strand probe which contained pNCA sequences from the *Msc*I site (position 662) 3′ of the PBS to the *Asp*718 site (position 481) in U5. Protection of the wild-type SF species did not produce any bands, as expected, because most of its genomic RNA had been degraded (Fig. 8B, lane 10). Protection of the FF species from Δ5E resulted in an approximately 130-nt species, corresponding to complete protection of the pNCA sequence of our probe (Fig. 8B, lane 11). Two bands were seen with Δ5E, suggesting that some RNA breakdown might be occurring. Protection of the VFF species from H7 resulted in an approximately 67-nt species (Fig. 8B,lane 12). All together, this suggests that the VFF species is actually a prematurely terminated minus-strand strong-stop DNA species, about 67 nt in length, resulting from RT pausing after the addition of approximately 49 nt to the 18-nt tRNA primer. H7 is able to polymerize past the pause site and produce low levels of full-length minus-strand strong-stop DNA. ΔC RT, however, appears to pause even more severely than H7, synthesizing almost entirely the truncated species.

The presence of the VFF species in wild-type virions treated with RNase A in high salt concentrations suggests that this marks a common pause site of M-MuLV RT. D524N synthesized strictly the FF or full-length minus-strand strong-stop DNA species, suggesting that while this RNase H was inactive, processive polymerization was unaffected. Y586F synthesized low levels of the VFF species. However, it made predominantly full-length FF minus-strand strong-stop DNA (Fig. 7B, lanes 9 to 11). Thus, the wild type, D524N, Y586F, and Δ5E are able to polymerize through this pause site and produce predominantly full-length minus-strand strong-stop DNA, suggesting that reduced RNase H activity does not necessarily result in increased RT pausing. Closer examination of long-time-frame endogenous reactions (Fig. 4) shows an accumulation of a truncated species migrating at approximately 67 nt.

To determine whether the VFF species produced by H7 and ΔC was single or double stranded, we again eluted it and subjected it to S1 nuclease digestion (Fig. 6 and data not shown). The VFF species was resistant to S1 digestion, producing an approximately 67-bp doublet (Fig. 6, lanes 15 and 16). This suggests that this truncated DNA is in hybrid form with the genomic RNA. As H7 is an RNase H null mutant, this result was not unexpected. However, as ΔC had wild-type RNase H activity in vitro, its inability to degrade its genomic RNA was surprising.

Further analysis of strand translocation by RNase H mutants. To assay strand translocation quantitatively, we developed an additional assay. We performed the endogenous reaction in the presence of 2 mM nonradiolabeled deoxyribonucleotides, treated the reaction mixture with 0.33 N NaOH for 30 min at 55°C to remove all remaining RNA, and then

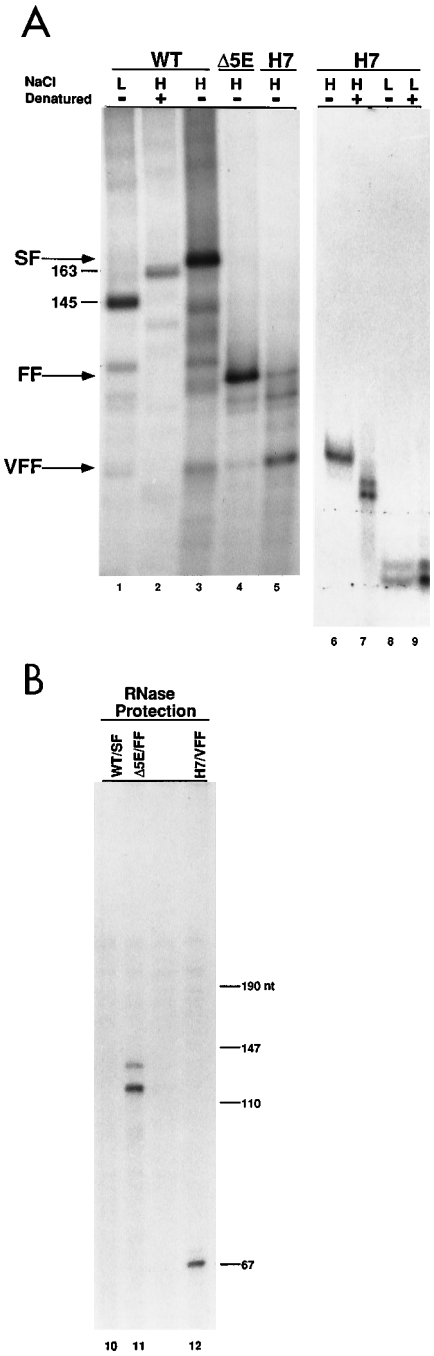

FIG. 8. RNase A treatment in high and low salt concentrations and RNase protection of plus-strand RNA from endogenous reaction products. (A) The endogenous reaction was performed as described in Materials and Methods with 2.5 μM [α-^{32}P]TTP at 400 Ci/mmol. WT, wild type. The products were treated with RNase A in high (H) or low (L) salt concentrations prior to electrophoresis on 7.5% nondenaturing polyacrylamide gels. Lane 2 was denatured prior to loading by suspension in dye containing formamide; lanes 1 and 3 to 5 were analyzed without denaturation. The gel was exposed wet to X-ray film overnight. The VFF species from H7 in lane 5 was excised from the wet gel, electroeluted, ethanol precipitated, and then re-treated with RNase A in high and low salt concentrations. Lanes 7 and 9 were denatured prior to loading; lanes 6 and 8 were analyzed without denaturation. (B) The WT/SF, Δ5E/FF, and H7/VFF species were excised from the wet gel used for panel A, electroeluted, ethanol precipitated, and then treated with DNase I to remove the radiolabeled minus-strand DNA. The remaining plus-strand genomic RNA was RNase protected by standard techniques with a minus-strand probe which contained pNCA sequences from an *Msc*I site (position 662) 3′ of the PBS to an *Asp*718 site (position 481) in U5 and analyzed on a 7.5% denaturing polyacrylamide gel.

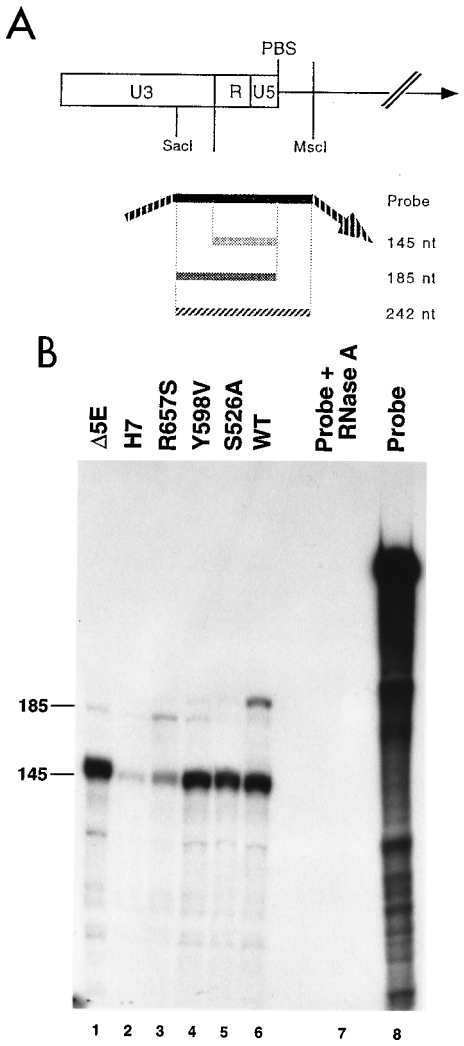

FIG. 9. Reverse transcription in vitro in the endogenous reaction. (A) Diagram of the RNase protection probe, spanning pNCA sequences from *Sac*I (position 414) to *Msc*I (position 662) in pNCA, which includes the U5 and R regions and part of the U3 region of the M-MuLV long terminal repeat. Protection differentiates between minus-strand strong-stop DNA (145 nt), translocated products (185 nt), and full-length complete minus-strand DNA (245 nt). (B) The endogenous reaction was performed with nonradiolabeled 2 mM TTP and was followed by RNase protection with the probe as described for panel A. WT, wild-type pNCA.

performed an RNase protection assay for the minus-strand DNAs. Our radiolabeled probe contained pNCA sequences from the *Sac*I site (position 414) in U3 to the *Msc*I site (position 662) 3′ of the PBS. Protection with this probe allows differentiation between minus-strand strong-stop DNA (145 nt), translocated species (185 nt), and full-length minus-strand DNA (242 nt; Fig. 9). The wild type was able to efficiently translocate, protecting both a 145-nt species and a 185-nt translocated species (Fig. 9B, lane 6). In the endogenous assay, it is difficult to observe full-length minus-strand DNA during the time course of the reaction, and the 242-nt species is not detected in this in vitro assay. RNase protection of the RNase H null mutants, Δ5E and H7, resulted in the protection of only the 145-nt species (Fig. 9B, lanes 1 and 2), confirming that these mutants cannot translocate their minus-strand strong-stop DNA.

Mutant H7 was reduced in overall minus-strand strong-stop

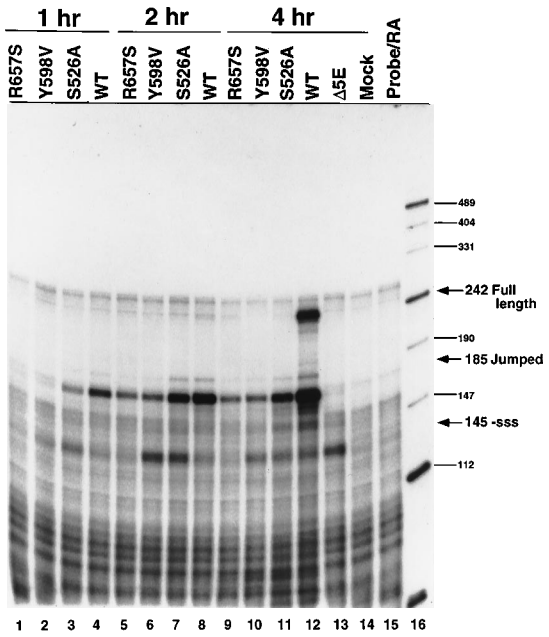

FIG. 10. RNase protection of low-molecular-weight, preintegrative viral DNA. Low-molecular-weight, preintegrative DNA was harvested at 1, 2, and 4 h postinfection and subjected to RNase protection with the probe described in the legend to Fig. 9A. WT, wild-type pNCA; Mock, mock-infected NIH 3T3 control; Probe/RA, probe plus RNase; −sss, minus-strand strong-stop DNA. Numbers on the right represent sizes in nucleotides.

DNA levels (Fig. 9B, lane 2). This reduction probably results from decreased processivity and increased polymerase pausing by RT, as addressed previously (62). R657S was also reduced in the amount of minus-strand strong-stop DNA detected, suggesting that R657S also is impaired in DNA synthesis (Fig. 9B, lane 3). RNase protection of R657S appears to produce a translocated species shorter than the 185-nt species protected by the wild type. This band can be detected upon longer exposures for the other mutants and the wild type, but this translocated species is present at almost the same level as minus-strand strong-stop DNA for R657S. Thus, the reduction in the levels of longer minus-strand products synthesized for R657S in the endogenous reaction probably results from reduced polymerization, rather than reduced strand transfer.

Mutants Y598V and S526A also showed little translocated DNA, although significant minus-strand strong-stop DNA levels were detected (Fig. 9B, lanes 4 and 5). These mutants appear to be fully competent RNases H, leaving their minus-strand strong-stop DNA in single-stranded form, and so this lack of translocation presumably does not result from hybrid minus-strand strong-stop DNA. We tested various Nonidet P-40 concentrations (0.5 to 0.05%) to determine whether this lack of translocation might be due to subtle in vitro-induced perturbations of the capsid which these mutants could not withstand. We did not see any markedly increased translocation under any of these conditions (data not shown). When the endogenous reaction was performed for even longer times, we were able to detect some longer minus-strand products. Thus, in vitro these two mutants seem to synthesize minus-strand strong-stop DNA as well as the wild type and to degrade their genomic RNA from this minus-strand strong-stop DNA, but they are specifically delayed in first-strand translocation.

Strand translocation in vivo. To examine translocation in vivo, low-molecular-weight, preintegrative DNA from the wild type, S526A, R657S, Y598V, and Δ5E was harvested from NIH 3T3 cells at 1, 2, or 4 h postinfection and analyzed by RNase protection assays (Fig. 10). We used the probe described previously, which was able to differentiate between minus-strand strong-stop DNA (145 nt), translocated DNA (185 nt), and full-length minus-strand DNA (242 nt; Fig. 9A). With wild-type virus, translocated DNA was seen at very early time points, and full-length DNA was seen within several hours, suggesting that translocation and reverse transcription occur very rapidly in vivo (Fig. 10, lanes 4, 8, and 12). We did not detect protection of the 145-nt species for the wild type at any time point, suggesting that the wild type elongates and translocates very efficiently, never allowing minus-strand strong-stop DNA to accumulate to detectable levels.

In contrast, we could detect the 145-nt species after infection with the RNase H null mutant Δ5E (Fig. 10, lane 13). In vitro, this mutant is unable to translocate, and analysis of its minus-strand strong-stop DNA has demonstrated that this DNA remains in hybrid form with the genomic RNA. This suggests that minus-strand strong-stop DNA accumulates to detectable levels in vivo only if not efficiently translocated and that it is not a species generated to significant levels during wild-type reverse transcription in vivo, as it is in vitro during the endogenous reaction. In vivo, reverse transcription and strand translocation in particular appear more efficient.

The translocated 185-nt species could be weakly seen with mutant R657S at 2 and 4 h postinfection (Fig. 10, lanes 5 and 9). The overall levels of translocated DNA appeared reduced for this mutant, supporting the in vitro observation from the endogenous reaction that this mutant is impaired in DNA synthesis. However, similar to the case with the wild type, we did not detect any of the 145-nt species with this mutant, suggesting that it is able to translocate efficiently the minus-strand strong-stop DNA which it is able to synthesize.

With mutants Y598V and S526A, however, we were able to detect minus-strand strong-stop DNA at 1 and 2 h postinfection (Fig. 10, lanes 2, 3, 6, and 7). These mutants appear to synthesize minus-strand strong-stop DNA but then to be stalled, allowing this species to accumulate. As these mutants leave their minus-strand strong-stop DNA in single-stranded form, this accumulation is not due to hybrid minus-strand strong-stop DNA, as is the case for Δ5E. Rather, they appear to be impaired specifically in strand transfer, independent of their ability to degrade genomic RNA. Translocated species appear with a delay compared with the wild type.

DISCUSSION

Many of the mutant RNases H examined in this study retained significant RNA-DNA nuclease activity in vitro (5) but were replication defective in vivo. The results suggest the existence of various classes of RNase H mutants, discussed in detail below.

RNase H mutants unable to degrade genomic RNA. Four of the RNase H mutants, D524N, Y586F, Δ5E, and ΔC, were unable to degrade their genomic RNA, and thus their minus-strand strong-stop DNA remained in hybrid form, preventing the requisite base pairing between complementary R regions believed to facilitate first-strand translocation. D524N, Y586F, and Δ5E all synthesize predominantly full-length minus-strand strong-stop DNA, and it can be inferred that their lack of translocation results from the hybrid nature of this DNA. D524N and Y586F had the most easily explained phenotypes: they had little RNase H activity in vitro, consistent with the hybrid minus-strand strong-stop DNA detected in the endogenous reaction. ΔC made only short DNA products, indicating

additional elongation defects. Interestingly, ΔC and Δ5E had considerable RNase H activity in vitro as assayed by in situ gel techniques. These results suggest that these two mutants have problems only apparent under in vivo conditions. We believe that this discrepancy may be explained by the different divalent cations used in these two assays (6).

RNase H mutants affecting DNA elongation. Two mutants, ΔC and H7, showed an increase in pausing by RT during DNA elongation. These two mutants produced predominantly shorter products during the early stages of reverse transcription, and little or no full-length minus-strand strong-stop DNA was detected. They appeared to pause prematurely after the addition of approximately 49 nt following tRNA initiation, producing a 67-nt minus-strand species, VFF (49 nt plus the 18-nt tRNA primer). We believe that these species are tRNA primed because they shift to a species approximately 18 nt smaller upon treatment with RNase A in low salt concentrations, i.e., under conditions which permit degradation of all genomic RNA. While even the wild type appears to weakly pause here, ΔC and H7 are not able to polymerize efficiently past the pause site, exhibiting the most severe pausing defect of all the RNase H mutants analyzed. We cannot definitively explain why the double-stranded VFF species produced by RNase A treatment in high salt concentrations (Fig. 8A, lane 6) migrates more slowly than the denatured VFF species (Fig. 8A, lane 7). It is interesting that this VFF species, also detected at low levels in the replication products of the wild type and other mutants, is double stranded and not yet degraded by RNase H. This may suggest that RNase H cleavage and DNA synthesis are not always tightly coupled and that RNase H does not always digest the hybrid even when up to 50 nt have been added.

H7 is a linker insertion mutant which causes a frameshift between the DNA polymerase and RNase H domains and is thus effectively a ΔRH form of RT. ΔC has lost the 11-amino-acid C helix. Previous in vitro characterization of bacterially expressed ΔC and ΔRH showed that these two mutants made shorter products on both homopolymeric and heteropolymeric substrates (62). That report suggested that this reduced processivity might result in an increase in prematurely paused products in vivo during replication, and our results are consistent with this prediction. As that report characterized mutant RTs on DNA primer templates, our work extends this result to RNA primer templates in vivo, even in the presence of additional viral proteins, such as NC, which might have influenced processive synthesis (1, 22, 41).

The other RNase H mutants which we tested appeared to pause to different extents. Δ5E and D524N did not appear to pause significantly, suggesting that the absence of RNase H activity does not necessarily result in increased RT pausing. Y586F produced predominantly full-length minus-strand strong-stop DNA, pausing slightly. R657S appears to pause more than either Δ5E or D524N, but it is a fully active RNase H, as evidenced by the single-stranded minus-strand strong-stop DNA detected in the endogenous reaction (Fig. 4A, lane 1). This suggests that increased RT pausing may reflect a structural, rather than enzymatic, RNase H-mediated effect on DNA polymerase activity. It has been suggested that the RNase H domain is necessary for efficient substrate binding by RT, perhaps through the C helix. This basic region may ordinarily stabilize enzyme-substrate interactions. Replacement of the positively charged residues in this region in the *E. coli* enzyme decreased the enzyme's affinity for substrate without affecting the rate of RNA hydrolysis (38). Previously, on the basis of our in vitro analysis of R657S, we hypothesized that this mutant might perturb a point of interaction between the DNA polymerase and the RNase H domains (5). Taken together, these ideas suggest that an intact RNase H domain may provide necessary enzyme contacts with the substrate to allow efficient, processive DNA synthesis. Previous work has suggested that wild-type RT forms a dimer when bound to a primer template during polymerization and that ΔC and ΔRH are unable to form a similar dimer under polymerization conditions (62). The connection between dimer formation and processive DNA synthesis remains unclear, but it is suggestive evidence of a structural RNase H-mediated effect on DNA processivity.

Others have invoked a more direct role for RNase H activity in augmenting DNA processivity and suggest that the inability of RNase H to hydrolyze the RNA template may create blocks to further synthesis by reducing the rates of DNA polymerization at these paused positions (19, 20). These authors observed an increase in polymerase pausing with the HIV-1 equivalent of mutant D524N, D443N, on heteropolymeric substrates in vitro. While we did not see significant decreased processivity in the endogenous reaction for D524N, there is some evidence that in vitro on heteropolymeric templates this mutant is less processive than the wild type (62). The presence of other aspects of the capsid environment may increase the processivity of this mutant in our assays and in vivo, where RNase H activity per se does not seem to be the critical factor in permitting processive DNA synthesis.

RNase H mutants affecting strand translocation. Two RNase H mutants showed a remarkable phenotype: they were specifically defective in first-strand transfer. Our results suggest that they are able to synthesize minus-strand strong-stop DNA as efficiently as the wild type but that where the wild type translocates, these mutants are stalled. Further, Y598V and S526A were able to degrade the template RNA from their minus-strand strong-stop DNA as well as the wild type. The extent of first-strand translocation, however, for these mutants was severely reduced both in the endogenous reaction in vitro and in vivo. This translocation defect is not merely a phenotype seen for all RNase H mutants, but a defect specific to these two mutants. These mutants thus define a novel function for the RNase H domain, i.e., specifically participating in the translocation process itself.

The role of RNase H in strand transfer has been analyzed in vitro, by using purified recombinant enzymes and templates designed to mimic the in vivo process (18, 24, 44, 51). In vitro, transfer reactions appear to be dependent on the concentration of the two templates, suggesting that the rate-limiting step in strand transfer involves the interaction of the elongated DNA with the acceptor template. In general, transfer is enhanced in vitro under conditions of acceptor-to-donor excess. Several groups have observed a reduction in strand transfer efficiencies when using an RNase H-minus form of RT, supporting RNase H's role in strand transfer (18, 24, 44, 51). In these studies it was concluded that RNase H's degradation of the donor RNA facilitated translocation, but it was difficult to address whether RNase H was additionally involved in strand transfer. Analysis of RNase H's role in strand transfer has often used a truncated ΔRH form (18), which may have complicated analysis because of this RT's additional problems, such as increased pausing and decreased processivity (61, 62). The presence of the RNase H structure and its potential interactions with the DNA polymerase domain may be critical for strand translocation.

Analysis of the mutants Y598V and S526A is not complicated by additional defects. The presence of the strand transfer defect for these mutants suggests that RNase H has an additional role in translocation, independent of its ability to de-

grade genomic RNA. This defect may reflect the effect of structural alterations imposed by the mutations on RT, including subtle effects on the DNA polymerase domain or DNA polymerase activity by the RNase H domain. While the first-strand transfer is often thought of as the first "jump," the minus-strand strong-stop DNA–RT complex may not actually separate from the donor PBS template. Strand transfer may be facilitated by the binding of the DNA polymerase domain to the acceptor and that of the RNase H domain to the donor, in order to bridge the transition between templates. Y598V and S526A may have either altered RT's affinity for its substrate or altered the orientation between the DNA polymerase and RNase H domain which may be essential to transfer efficiently between templates. It has been suggested that the RNase H domain of HIV-1 RT contributes to RT's affinity for templates greater than 14 nt (8, 16, 23, 69). It is interesting that Y598V alters a conserved residue in M-MuLV RT's C helix, a region which has been implicated in substrate binding for both the M-MuLV and *E. coli* enzymes (38).

A long-standing question in retrovirology has been whether the actions of DNA polymerase and RNase H are coordinated during reverse transcription. It has been suggested that the two activities are functionally uncoupled and that a second RT may be involved in degrading the genomic RNA after DNA synthesis is complete (17, 33). Using phenotypically mixed virions, Telesnitsky and Goff (63) demonstrated that DNA synthesis could be completed when the DNA polymerase and RNase H activities were provided by separate molecules. However, all pairs of DNA polymerase and RNase H mutants did not complement, including several combinations of mutants which appeared to retain significant DNA polymerase and RNase H activity (63). This is consistent with the emerging model that even though an RNase H mutant may be able to degrade RNA, it may be perturbed in other specialized functions, such as strand transfer, which are essential for efficient reverse transcription.

An alternative explanation for the failure of S526A and Y598V to mediate translocation is that these mutants might leave aberrant amounts of RNA annealed to the 3′ end of the minus-strand strong-stop DNA, which might inhibit strand transfer. However, we were not able to detect any differences in the RNA which remained associated with the minus-strand strong-stop DNA compared with the wild type, and we did not observe any differences in the state of the minus-strand strong-stop DNA by either S1 nuclease analysis or RNase A treatment in high salt concentrations. It has been suggested that RNase H cannot degrade the extreme 5′ end of the genomic RNA template because of spacing restrictions imposed by the distance between the DNA polymerase and RNase H active sites and that RNase H may leave between 7 and 17 nt of RNA annealed to the 3′ end of the minus-strand strong-stop DNA (4, 21, 23, 48, 56). How this bit of genomic RNA is removed, if at all, is unknown. An unwinding activity for avian myeloblastosis virus RT, which breaks base pairing in both RNA-DNA and DNA-DNA duplexes, has been described previously (7, 13, 32). This activity may be involved in the dissociation of RNA hybridized to the 3′ terminus of the minus-strand strong-stop DNA, thereby generating the free end for the requisite base pairing with the 3′ end of the genomic RNA. It is conceivable that Y598V and S526A may have perturbed this activity. It is also possible that strand transfer occurs from R regions internal to the 3′ end, and in this scenario the problem of removing any remaining 5′ RNA is actually a moot point. Two groups have shown that markers in R region sequences can be lost during reverse transcription, implying that transfer can occur before minus-strand strong-stop DNA synthesis is completed (43, 52).

We did not detect significant minus-strand strong-stop DNA in vivo with wild-type virus, implying that this species does not normally accumulate in the cell, but rather is efficiently translocated and extended. The abundant levels of minus-strand strong-stop DNA detected in vitro during the endogenous reaction suggest that this assay is somewhat artificial and that some aspect of the transfer process has been disrupted. This observation supports previous results which suggested that the abundant minus-strand strong-stop DNA levels seen in vitro may not actually be detected in vivo (42, 58, 65, 66). It has been suggested that the minus-strand strong-stop DNA synthesized during the endogenous reaction may actually be an abortive species, because of the addition of one extra nontemplated base at the 3′ end of the DNA, which might inhibit strand transfer (58). Nontemplated base addition has also been observed for HIV-1 RT in reconstituted strand transfer reactions, as well as for other DNA polymerases when they pause at the end of templates (10, 50, 51). Thus, it is conceivable that the minus-strand strong-stop DNA which we detect in vivo for the translocation-defective mutants is also an abortive species and that only the small percentage of minus-strand DNA which is transferred directly actually will be completed and integrated.

Three mutants, Q530N, AQ558NN, and FL625GA, which had wild-type DNA polymerase and RNase H activity in vitro, were completely infectious in vivo. While residues Q-530, A-558, and A-559 have been implicated in substrate binding, mutation of these residues did not seem to affect either RNase H activity in vitro or viral replication in vivo (37, 38, 47).

In conclusion, this work lends credence to the idea that the DNA polymerase and RNase H activities of RT are more intricately connected during the course of reverse transcription than was previously thought. In addition to its essential role in the degradation of the genomic RNA, RNase H is involved in DNA elongation and strand translocation.

ACKNOWLEDGMENTS

We thank W. Yang, W. Hendrickson, and A. Telesnitsky for helpful discussion; A. Telesnitsky for an RNase protection plasmid; K. Alin for help with Southern blot analysis; and K. de los Santos for help with the construction of M-MuLV proviral plasmids.

This work was supported by Public Health Service grant CA 30488 from the National Cancer Institute and the Howard Hughes Medical Institute. Support for S.W.B. was provided by a PHS Predoctoral Training Grant from the NIGMS. S.P.G. is an Investigator of the Howard Hughes Medical Institute.

REFERENCES

1. **Allain, B., M. Lapadat-Tapolsky, C. Berlioz, and J.-L. Darlix.** 1994. Transactivation of the minus strand DNA transfer by nucleocapsid protein during reverse transcription of the retroviral genome. EMBO J. **13:**973–981.
2. **Baltimore, D.** 1970. RNA-dependent DNA polymerase in virions of RNA tumor viruses. Nature (London) **226:**1209–1211.
3. **Bavand, M. R., R. Wagner, and T. J. Richmond.** 1993. HIV-1 reverse transcriptase: polymerization properties of the p51 homodimer compared to the p66/p51 heterodimer. Biochemistry **32:**10543–10552.
4. **Ben-Artzi, H., E. Zeelon, B. Amit, A. Wortzel, M. Gorecki, and A. Panet.** 1993. RNase H activity of reverse transcriptases on substrates derived from the 5′ end of retroviral genome. J. Biol. Chem. **268:**16465–16471.
5. **Blain, S. W., and S. P. Goff.** 1993. Nuclease activities of Moloney murine leukemia virus reverse transcriptase: mutants with altered substrate specificities. J. Biol. Chem. **268:**23585–23592.
6. **Blain, S. W., and S. P. Goff.** Unpublished results.
7. **Boone, L. R., and A. M. Skalka.** 1981. Viral DNA synthesized in vitro by avian retrovirus particles permeabilized with melittin. II. Evidence of a strand displacement mechanism in plus-strand synthesis. J. Virol. **37:**117–126.
8. **Boyer, P. L., A. L. Ferris, and S. H. Hughes.** 1992. Mutational analysis of the fingers domain of human immunodeficiency virus type 1 reverse transcriptase. J. Virol. **66:**7533–7537.
9. **Champoux, J. J.** 1993. Roles of ribonuclease H in reverse transcription, p. 103–118. *In* A.-M. Skalka and S. P. Goff (ed.), Reverse transcriptase. Cold

Spring Harbor Laboratory, Cold Spring Harbor, N.Y.
10. **Clark, J. M.** 1988. Novel non-templated nucleotide addition reactions catalyzed by procaryotic and eucaryotic DNA polymerases. Nucleic Acids Res. **16:**9677–9686.
11. **Coffin, J. M., and W. A. Haseltine.** 1977. Terminal redundancy and the origin of replication of Rous sarcoma virus RNA. Proc. Natl. Acad. Sci. USA **74:**1908–1912.
12. **Colicelli, J., and S. P. Goff.** 1988. Sequence and spacing requirements of a retrovirus integration site. J. Mol. Biol. **199:**47–59.
13. **Collett, M. S., J. P. Leis, M. S. Smith, and A. J. Faras.** 1978. Unwinding-like activity associated with avian retrovirus RNA-directed DNA polymerase. J. Virol. **26:**498–509.
14. **Crouch, R. J.** 1990. Ribonuclease H: from discovery to 3D structure. New Biol. **2:**771–777.
15. **Davies, J. F., II, Z. Hostomska, Z. Hostomsky, S. R. Jorden, and D. A. Matthews.** 1991. Crystal structure of the ribonuclease H domain of HIV-1 reverse transcriptase. Science **252:**88–95.
16. **DeStefano, J. J., R. A. Bambara, and P. J. Fay.** 1993. Parameters that influence the binding of human immunodeficiency virus reverse transcriptase to nucleic acid structures. Biochemistry **32:**6908–6915.
17. **DeStefano, J. J., R. G. Buiser, L. M. Mallaber, T. W. Myers, R. A. Bambara, and P. J. Fay.** 1991. Polymerization and RNase H activities of the reverse transcriptases from avian myeloblastosis, human immunodeficiency, and Moloney murine leukemia viruses are functionally uncoupled. J. Biol. Chem. **266:**7423–7431.
18. **DeStefano, J. J., L. M. Mallaber, L. Rodriguez-Rodriguez, P. J. Fay, and R. A. Bambara.** 1992. Requirements for strand transfer between internal regions of heteropolymer templates by human immunodeficiency virus reverse transcriptase. J. Virol. **66:**6370–6378.
19. **Dudding, L. R., and V. Mizrahi.** 1993. Rapid kinetic analysis of a point mutant of HIV-1 reverse transcriptase lacking ribonuclease H activity. Biochemistry **32:**6116–6120.
20. **Dudding, L. R., N. C. Nkabinde, and V. Mizrahi.** 1991. Analysis of the RNA- and DNA-dependent DNA polymerase activities of point mutants of HIV-1 reverse transcriptase lacking ribonuclease H activity. Biochemistry **30:**10498–10506.
21. **Fu, T.-B., and J. Taylor.** 1992. When retroviral reverse transcriptases reach the end of their RNA templates. J. Virol. **66:**4271–4278.
22. **Fuetterer, J., and T. Hohn.** 1987. Involvement of nucleocapsids in reverse transcription: a general phenomenon? Trends Biochem. Sci. **12:**92–95.
23. **Furfine, E. S., and J. E. Reardon.** 1991. Reverse transcriptase-RNase H from the human immunodeficiency virus: relationship of the DNA polymerase and RNA hydrolysis activities. J. Biol. Chem. **266:**406–412.
24. **Garces, J., and R. Wittek.** 1991. Reverse-transcriptase-associated RNase H activity mediates template switching during reverse transcription *in vitro*. Proc. R. Soc. Lond. Ser. B Biol. Sci. **243:**235–239.
25. **Gilboa, E., S. W. Mitra, S. P. Goff, and D. Baltimore.** 1980. A detailed model of reverse transcription and tests of crucial aspects. Cell **18:**93–100.
26. **Goff, S. P.** 1990. Retroviral reverse transcriptase: synthesis, structure and function. J. Acquired Immune Defic. Syndr. **3:**817–831.
27. **Goff, S. P., P. Traktman, and D. Baltimore.** 1981. Isolation and properties of Moloney murine leukemia virus mutants: use of a rapid assay for release of virion reverse transcriptase. J. Virol. **38:**239–248.
28. **Hartman, S. C., and R. C. Mulligan.** 1988. Two dominant acting selectable markers for gene transfer in mammalian cells. Proc. Natl. Acad. Sci. USA **85:**8047–8051.
29. **Hirt, B.** 1967. Selective extraction of polyoma DNA from infected mouse cell cultures. J. Mol. Biol. **106:**365–369.
30. **Hu, S. C., D. L. Court, M. Zweig, and J. G. Levin.** 1986. Murine leukemia virus *pol* gene products: analysis with antisera generated against reverse transcriptase and endonuclease fusion proteins expressed in *Escherichia coli*. J. Virol. **60:**267–274.
31. **Hu, W.-S., and H. M. Temin.** 1990. Retroviral recombination and reverse transcription. Science **250:**1227–1233.
32. **Huber, H. E., J. M. McCoy, J. S. Seehra, and C. C. Richardson.** 1989. Human immunodeficiency virus 1 reverse transcriptase. Template binding, processivity, strand displacement synthesis, and template switching. J. Biol. Chem. **264:**4669–4678.
33. **Huber, H. E., and C. C. Richardson.** 1990. Processing the primer for plus strand DNA synthesis by human immunodeficiency virus 1 reverse transcriptase. J. Biol. Chem. **265:**10565–10573.
34. **Jacobo-Molina, A., and E. Arnold.** 1991. HIV reverse transcriptase structure-function relationships. Biochemistry **30:**6354–6361.
35. **Jacobo-Molina, A., J. Ding, R. G. Nanni, A. D. J. Clark, X. Lu, C. Tantillo, R. L. Williams, G. Kamer, A. L. Ferris, P. Clark, A. Hizi, S. H. Hughes, and E. Arnold.** 1993. Crystal structure of human immunodeficiency virus type 1 reverse transcriptase complexed with double-stranded DNA at 3.0 A resolution shows bent DNA. Proc. Natl. Acad. Sci. USA **90:**6320–6324.
36. **Jones, J. S., R. W. Allan, and H. M. Temin.** 1994. One retroviral RNA is sufficient for synthesis of viral DNA. J. Virol. **68:**207–216.
37. **Kanaya, S., C. Katsuda, S. Kimura, T. Nakai, E. Kitakuni, H. Nakamura, K. Katayanagi, K. Morikawa, and M. Ikehara.** 1991. Stabilization of *Escherichia coli* ribonuclease H by introduction of an artificial disulfide bond. J. Biol. Chem. **266:**6038–6044.
38. **Kanaya, S., C. Katsuda-Nakai, and M. Ikehara.** 1991. Importance of the positive charge cluster in *Escherichia coli* ribonuclease H1 for the effective binding of substrate. J. Biol. Chem. **266:**11621–11627.
39. **Katayanagi, K., M. Miyagawa, M. Matsushima, M. Ishikawa, S. Kanaya, M. Ikehara, T. Matsuzaki, and K. Morikawa.** 1990. Three-dimensional structure of ribonuclease H from *E. coli*. Nature (London) **347:**306–309.
40. **Kohlstaedt, L. A., J. Wang, J. M. Friedman, P. A. Rice, and T. A. Steitz.** 1992. Crystal structure at 3.5 A resolution of HIV-1 reverse transcriptase complexed with an inhibitor. Science **256:**1783–1790.
41. **Lapadat-Tapolsky, M., H. De Rocquigny, D. van Gent, B. Roques, R. Plasterk, and J.-L. Darlix.** 1993. Interaction between HIV-1 nucleocapsid protein and viral DNA may have important functions in the viral life cycle. Nucleic Acids Res. **21:**831–839.
42. **Lee, Y. M. H., and J. M. Coffin.** 1991. Relationship of avian retrovirus DNA synthesis to integration in vitro. Mol. Cell. Biol. **11:**1419–1430.
43. **Lobel, L. I., and S. P. Goff.** 1985. Reverse transcription of retroviral genomes: mutations in the terminal repeats. J. Virol. **53:**447–455.
44. **Luo, B., and J. Taylor.** 1990. Template switching by reverse transcriptase during DNA synthesis. J. Virol. **64:**4321–4328.
45. **McCutchan, J. H., and J. S. Pagano.** 1968. Enhancement of the infectivity of simian virus 40 deoxyribonucleic acid with diethylaminoethyl-dextran. J. Natl. Cancer Inst. **41:**351–357.
46. **Nakamura, H., K. Katayanagi, K. Morikawa, and M. Ikehara.** 1991. Structural models of ribonuclease H domains in reverse transcriptases from retroviruses. Nucleic Acids Res. **19:**1817–1823.
47. **Nakamura, H., Y. Oda, S. Iwai, H. Inoue, E. Ohtsuka, S. Kanaya, S. Kimura, C. Katsuda, K. Katayanagi, K. Morikawa, H. Miyashiro, and M. Ikehara.** 1991. How does RNase H recognize a DNA-RNA hybrid? Proc. Natl. Acad. Sci. USA **88:**11535–11539.
48. **Oyama, F., R. Kikuchi, R. J. Crouch, and T. Uchida.** 1989. Intrinsic properties of reverse transcriptase in reverse transcription: associated RNase H is essentially regarded as an endonuclease. J. Biol. Chem. **264:**18808–18817.
49. **Panganiban, A. T., and D. Fiore.** 1988. Ordered interstrand and intrastrand DNA transfer during reverse transcription. Science **241:**1064–1069.
50. **Patel, P. H., and B. D. Preston.** 1994. Marked infidelity of human immunodeficiency virus type 1 reverse transcriptase at RNA and DNA template ends. Proc. Natl. Acad. Sci. USA **91:**549–553.
51. **Peliska, J. A., and S. J. Benkovic.** 1992. Mechanism of DNA strand transfer reactions catalyzed by HIV-1 reverse transcriptase. Science **258:**1112–1118.
52. **Ramsey, C. A., and A. T. Panganiban.** 1993. Replication of the retroviral terminal repeat sequence during in vivo reverse transcription. J. Virol. **67:**4114–4121.
53. **Rothenberg, E., and D. Baltimore.** 1977. Increased length of DNA made by virions of murine leukemia virus at limiting magnesium ion concentrations. J. Virol. **21:**168–178.
54. **Rothenberg, E., D. Smotkin, D. Baltimore, and R. A. Weinberg.** 1977. *In vitro* synthesis of infectious DNA of murine leukemia virus. Nature (London) **269:**122–126.
55. **Sambrook, J., E. F. Fritsch, and T. Maniatis.** 1989. Molecular cloning: a laboratory manual, 2nd ed. Cold Spring Harbor Laboratory, Cold Spring Harbor, N.Y.
56. **Schatz, O., J. Mous, and S. F. Le Grice.** 1990. HIV-1 RT-associated ribonuclease H displays both endonuclease and 3′-5′ exonuclease activity. EMBO J. **9:**1171–1176.
57. **Skalka, A.-M., and S. P. Goff, ed.** 1993. Reverse transcriptase. Cold Spring Harbor Laboratory, Cold Spring Harbor, N.Y.
58. **Swanstrom, R., H. E. Varmus, and J. M. Bishop.** 1981. The terminal redundancy of the retroviral genome facilitates chain elongation by reverse transcriptase. J. Biol. Chem. **256:**1115–1121.
59. **Tanese, N., and S. P. Goff.** 1988. Domain structure of the Moloney murine leukemia virus reverse transcriptase: mutational analysis and separate expression of the polymerase and RNase H activities. Proc. Natl. Acad. Sci. USA **85:**1777–1781.
60. **Tanese, N., A. Telesnitsky, and S. P. Goff.** 1991. Abortive reverse transcription by mutants of Moloney murine leukemia virus deficient in the reverse transcriptase-associated RNase H function. J. Virol. **65:**4387–4397.
61. **Telesnitsky, A., S. W. Blain, and S. P. Goff.** 1992. Defects in Moloney murine leukemia virus replication caused by a reverse transcriptase mutation modeled on the structure of *Escherichia coli* RNase H. J. Virol. **66:**615–622.
62. **Telesnitsky, A., and S. P. Goff.** 1993. RNase H domain mutations affect the interaction between Moloney murine leukemia virus reverse transcriptase and its primer-template. Proc. Natl. Acad. Sci. USA **90:**1276–1280.
63. **Telesnitsky, A., and S. P. Goff.** 1993. Two defective forms of reverse transcriptase can complement to restore retroviral infectivity. EMBO J. **12:**4433–4438.
64. **Temin, H. M., and S. Mizutani.** 1970. RNA-directed DNA polymerase in virions of Rous sarcoma virus. Nature (London) **226:**1211–1213.

65. **Varmus, H. E., and P. Brown.** 1989. Retroviruses, p. 55–108. *In* D. E. Berg and M. M. Howe (ed.), Mobile DNA. American Society for Microbiology, Washington, D.C.
66. **Varmus, H. E., S. Heasley, K.-J. Kung, H. Oppermann, W. C. Smith, J. M. Bishop, and P. R. Shank.** 1978. Kinetics of synthesis, structure and purification of avian sarcoma virus-specific DNA made in the cytoplasm of acutely infected cells. J. Mol. Biol. **120:**55–82.
67. **Wigler, M., R. Sweet, G. K. Sim, B. Wold, A. Pellicer, E. Lacy, T. Maniatis, S. Silverstein, and R. Axel.** 1979. Transformation of mammalian cells with genes from procaryotes and eucaryotes. Cell **16:**777–785.
68. **Wintersberger, U.** 1990. Ribonucleases H of retroviral and cellular origin. Pharmacol. Ther. **48:**259–280.
69. **Wohl, B. M., M. M. Georgiadis, A. Telesnitsky, W. A. Hendrickson, and S. F. J. LeGrice.** 1995. Footprint analysis of replicating murine leukemia virus reverse transcriptase. Science **267:**96–99.
70. **Yang, W., W. A. Hendrickson, R. J. Crouch, and Y. Satow.** 1990. Structure of ribonuclease H phased at 2 Å resolution by MAD analysis of the selenomethionyl protein. Science **249:**1398–1405.